Free Radical Research, January 2010, 44(1): 108–117

informa
healthcare

Anti-cancer activity of nitrones in the *Apc*$^{Min/+}$ model of colorectal cancer

ROBERT A. FLOYD[1,2], RHEAL A. TOWNER[3,4], DEE WU[5,6], ANDREW ABBOTT[3], REBECCA CRANFORD[3], DAN BRANCH[3], WEI-XING GUO[1], STEVEN B. FOSTER[7], INNA JONES[3], RAJIB ALAM[5], DANNY MOORE[8], TOBY ALLEN[8] & MARK HUYCKE[8,9]

[1]*Experimental Therapeutics Research Program, Oklahoma Medical Research Foundation, Oklahoma City, OK 73104, USA,* [2]*Department of Biochemistry and Molecular Biology, University of Oklahoma Health Sciences Center, Oklahoma City, OK 73104, USA,* [3]*Advanced Magnetic Resonance Center, Oklahoma Medical Research Foundation, Oklahoma City, OK 73104, USA,* [4]*Departments of Pathology and Pharmaceutical Sciences,* [5]*Department of Radiological Sciences, University of Oklahoma Health Sciences Center, Oklahoma City, OK 73104, USA,* [6]*Computer Science,* [7]*Department of Chemistry, University of Oklahoma, Norman, OK 73069, USA,* [8]*The Muchmore Laboratories for Infectious Disease Research, Department of Veterans Affairs Medical Center, Oklahoma City, OK 73104, USA, and* [9]*Department of Medicine, University of Oklahoma Health Sciences Center, Oklahoma City, OK 73190, USA*

(Received date: 10 July 2009; in revised form date: 25 August 2009)

Abstract

The nitrones of α-phenyl-tert-butyl nitrone (PBN) and 4-hydroxyl-PBN (4-OH-PBN) that have anti-cancer activity in models of liver cancer and glioblastomas were tested in the ApcMin/+ mouse model. Mice were administered PBN and 4-OH-PBN in drinking water and intestinal tumour size and number assessed after 3–4 months. Throughout the experiment, contrast-enhanced magnetic resonance imaging (MRI) was used to monitor colon tumours. MRI data showed a time-dependent significant increase in total colonic signal intensity in sham-treated mice, but a significant decrease for PBN-treated mice and slight decrease for 4-OHPBN treated mice, probably due to the limited water solubility of 4-OH-PBN. Final pathological and percentage survival data agreed with the MRI data. PBN had little effect on oxaliplatin-mediated killing of HCT116 colon cancer cells and caused only a slight decrease in the amount of active fraction caspase 3 in oxaliplatin-treated cells. PBN has significant anti-cancer activity in this model of intestinal neoplasia.

Keywords: *Nitrones, HCT-116 cells, Apc*$^{Min/+}$ *mice, colorectal cancer, oxaliplatin*

Abbreviations: *CRC, colorectal cancer; PBN, a-phenyl-tert-butyl nitrone; MRI, magnetic resonance imaging; 4-OHPBN, 4-hydroxy-phenyl-tert-butyl nitrone; EPR, electron paramagnetic resonance; DMEM, Dulbecco's Modification of Eagle's Medium; MTS, 3-(4,5-dimethylthiozol-2-yl)-5(3-carboxymethoxyphenyl)-2H-tetrazoluim); Gd-DTPA, gadolinium-diethylenetriamine penta-acetic acid; iNOS, inducible Nitric Oxide Synthase; NO, nitric oxide.*

Introduction

Colorectal cancer (CRC) is the third leading cause of cancer death in the US, with an overall 5 year survival rate of only 65% [1]. Approximately half of the patients with CRC develop liver metastases—a complication that substantially contributes to mortality. Despite recent advances in therapy for advanced CRC, only limited survival advantages have been achieved [2]. There is an urgent need for novel therapeutics to augment current chemotherapeutic approaches, especially for metastatic disease. Nitrones are a class of compounds known for their ability to trap free radicals (R•) and offer potential as anti-cancer agents. These chemicals are typified by the general structure of

Correspondence: Dr Robert Floyd, 825 NE 13th St, Oklahoma City, Oklahoma 73104, USA. Tel: 4052717580. Email: robert-floyd@omrf.org

ISSN 1071-5762 print/ISSN 1029-2470 online
DOI: 10.3109/10715760903321796

X-CH=NO-Y where the nitrone moiety can form stable radical adducts (X-CHR=NO•-Y). Nitrones were recently noted to have potent anti-cancer activity in an animal model of liver cancer [3–6] and glioblastoma [7] but, to date, have not been studied in other cancer models to better define their promise.

Nitrones have been extensively used in electron paramagnetic resonance (EPR) to characterize short-lived free radicals [8]. For example, α-phenyl-*tert*-butyl-nitrone (PBN), a prototypic nitrone where X represents a phenyl moiety and Y a tert butyl group, can identify radicals by forming unique spin adducts [9]. After initial use of nitrones to identify radical intermediates in analytical chemistry, these compounds were subsequently found to be powerful tools for studying free radical intermediates in biochemical reactions [10–12] and whole animals [13–16].

The utility of nitrones in animal models led to the recognition that PBN has significant protective effects against ischemic stroke [3,17–19] and, in a few studies, against cancer [3,5–7,18]. Both of these diseases are believed to involve free radicals, although mechanisms for the therapeutic action of PBN may involve anti-inflammatory properties rather than radical trapping [18–20].

The preliminary observations on the potential anti-cancer activity of nitrones led us to consider the effect of PBN and 4-hydroxy-PBN (4-OH-PBN), a closely related nitrone, in the $Apc^{Min/+}$ model of intestinal neoplasia. This murine model harbours a germline mutation in *Apc* at codon 850 that leads to a truncation of the protein. Heterozygosity in one *Apc* allele occasionally generates the inactivation of the other allele by somatic recombination and when this occurs in intestinal epithelial cells adenomas form [21]. The molecular consequences of losing *Apc*, a multi-functional protein that binds microtubules, proteins in the Wnt/Wg pathway, α-catenin and axin, cytoskeletal regulators and the Rac guanine-nucleotide-exchange factor leads to the activation of β-catenin and induction of WNT signalling [22–24]. In $Apc^{Min/+}$ mice adenomas begin to develop in infancy, with death occurring at 16–20 weeks due to chronic intestinal haemorrhage [25,26]. Mice with this mutation on the C57BL/6 background develop an average of 30 small intestinal and five colonic adenomas per mouse. On occasion, adenomas progress to adenocarcinoma but metastases are not seen, most likely because mice do not live long enough for this late complication to occur.

In contrast to $Apc^{Min/+}$ mice, other murine models with targeted inactivation of *Apc* develop 10-fold more adenomas [27]. We selected the $Apc^{Min/+}$ model to investigate the effect of orally administered PBN and 4-OHPBN on tumour formation because the model has been used to study chemoprevention and relates well to human CRC [28–30]. We also applied magnetic resonance imaging (MRI) with gadolinium contrast to estimate *in vivo* rates of tumour change [31,32]. This imaging technique allowed us to collect time-dependent data on individual mice as treatments proceeded. Our results clearly show that PBN has potent chemopreventive activity in the $Apc^{Min/+}$ model. In addition, MRI findings indicated that PBN caused a time-dependent loss of total signal intensity, suggesting that this nitrone has a potential role as a therapeutic agent.

For chemotherapeutic agents to be effective they usually must be compatible with existing treatments. For mid- to late-stage CRC, after resection of the primary tumour and dissection of regional lymph nodes, adjunctive chemotherapy, when indicated, typically involves platinum-based agents [2]. Given this standard approach, we wanted to determine whether PBN interfered with oxaliplatin-induced killing of human cancer cells. *In vitro* testing using HCT116 human CRC cells demonstrated that PBN had no effect on oxaliplatin killing at concentrations considered effective in the $Apc^{Min/+}$ model. These findings demonstrate that nitrones are promising compounds for the prevention and/or treatment of colon adenomas and CRC.

Materials and methods

Synthesis of PBN and 4-OH-PBN

PBN and 4-OH-PBN were synthesized using a straightforward chemical reaction followed by an extraction and crystallization procedure as previously described [33]. PBN requires benzaldehyde and 2-methyl-2-nitro propane as starting chemicals, whereas 4-OHPBN utilizes 4-hydroxy-benzaldehyde in place of benzaldehyde. Nitrones synthesized in our laboratory have been characterized by mass spectroscopy, NMR and melting point analysis and found to be superior in terms of purity than commercially available nitrones.

Mouse breeding

Breeder pairs for C57BL/6J $Apc^{Min/+}$ mice were obtained from Jackson Laboratory (Bar Harbor, ME). The genotype of mice were confirmed by allele-specific PCR using DNA isolated from tail nicks and a kit supplied by Jackson Laboratory. At weaning mice were randomly assigned to one of three treatment groups consisting of untreated drinking water (sham) (n = 10) and drinking water to which PBN (n = 17) or 4-OHPBN (n = 19) was added. These compounds were administered at a rate of 100 mg/kg-day in drinking water. Water bottles were changed to fresh solutions twice weekly. Water consumption was assessed by weighing the water bottles to assure that PBN administration was ~ 100 mg/kg daily and that there was no difference in water consumption between experimental groups. Mice were group housed at five

per cage and fed lab chow *ad libitum*. All experiments involving mice were approved by the animal committee at OMRF and performed according to NIH guidelines on the use of experimental animals.

Enumeration of tumours

Necropsies were performed on mice when individual animals began to show signs of illness. To determine the number and size of tumours, small and large intestines were removed in their entirety, flushed with cold PBS and the small intestine divided into equal portions (proximal, mid and distal segments). All segments including colons were longitudinally opened, spread flat with the mucosal surface facing upward on black blotting paper and tumours immediately counted and measured to the nearest mm using a 10×-magnifying lens. Volumes were calculated assuming tumours were spherical in shape and using the diameter to calculate the tumour size.

Magnetic resonance imaging

MRI was performed using a Bruker Biospec 7.0 Tesla 30 cm bore horizontal small animal imaging system at the OMRF Small Animal MRI Core Facility. Gadolinium-enhanced MRI analysis was done on a sub-set of five mice in each group at four-to-six time points (variances due to MR imaging scheduling) during the experiment. To fully delineate the complex three-dimensional anatomy of the murine colon, we initially performed a luminal and tissue contrast-enhanced study on several mice. A Ferumoxide injectable solution (Feridex®) was instilled into the colon as a negative contrast agent and gadolinium injected intravenously as a positive contrast agent. For this pilot, the colon was surgically backfilled with Ferumoxide because timing the delivery of an orally administered contrast agent with intravenous gadolinium was considered difficult. Mice were anaesthetized with isoflurane and through a 5 mm midline abdominal incision the proximal colon was identified at its juncture to the cecum. Two ligatures 0.5 cm apart were loosely placed around the colon and a 2 mm incision made into the colon. A gavage needle was inserted and colon contents flushed per rectum using sterile PBS. The rectum was closed with a purse string ligature and the colon backfilled through the proximal colon incision with 1.0 ml of 1:10 dilution of Ferumoxide in saline. Both colonic ligatures were then tied to prevent backflow of the instilled contrast. The surgical area was washed with sterile PBS, the colon gently returned to the peritoneal cavity, the abdominal incision closed and mice allowed to recover. Gadolinium was then administered via a tail vein injection and serial gated transverse scans of the colon were performed from the upper abdomen to anus (~ 50 slices of 1 mm thickness). Only signal intensities from the colon were analysed as tumours in the small intestine were difficult to reliably identify.

For the remainder of the study, intravenous contrast-enhanced MRI, without Ferumoxide was performed on $Apc^{Min/+}$ mice to assess adenoma formation. MRI analysis was done on mice at ~ 7, 12, 16 and 18 weeks of age. Images were obtained using a multi-slice, multi-echo spin echo sequence with the following parameters: TR (repetition time) of 800 ms, TE (echo time) of 11.64 ms, two averages, a field-of-view of 30.88 mm × 17.49 mm, a matrix size of 256 × 171, a 1 mm slice thickness, 27 slices throughout the distal region, axial slice orientation and a spatial resolution of 121 × 102 mm^2/pixel. Initially, scout images were obtained to plan slices through the distal colon region (from kidneys to the rectum). Pre- and post-Gd-DTPA contrast agent administration was done (gadolinium diethylene triamine penta acetic acid; 0.2 mmol/kg, 110 µl volume via a tail-vein catheter). The post-contrast image was obtained 10 min following administration of Gd-DTPA.

For the signal intensity measurements, image analysis was done using Bruker Paravision 4.0 software. Regions of interest (ROIs) in the colon lumen (outer and inner contours) were delineated and the signal intensity due to Gd-DTPA measured using the ROI tool. An arbitrary area of normal muscle was outlined on each slice for referencing. Signal intensity values were added for all slices and referenced to the signal intensity of the dorsal back muscle. Average mean signal intensity (± SD) was obtained for each treatment group at different time-points. Trends by treatment group were estimated using linear equations for data fitting. Another independent group used perfusion maps to depict Gd-DTPA uptake in colon adenomas with pixel values outlined for analysis. The dynamic contrast enhancement (DCE-MRI) data were evaluated by a General Linear Model (GLM) to compare differences in slopes of mean signal intensity over time. Only data from 6–16 weeks were considered in the analysis since relatively few animals (particularly in the untreated group) survived beyond 16 weeks and inclusion of outlying data points would have inaccurately weighted their impact and biased results.

Percentage survival

Survival of each treatment group (untreated, PBN-treated and 4-OH-PBN-treated) were represented as the percentage of mice still surviving at given time points over the course of 156 days.

Cell culture

Stock cultures of HCT116 cells (ATCC) were grown in Dulbecco's Modification of Eagle's Medium

Table 1. Age and intestinal tumor multiplicity in $Apc^{Min/+}$ mice orally treated with nitrone compounds following weaning.

	Treatment groups (± SE)				
	Sham (n = 10)	4OH-PBN (n = 20)	PBN (n = 15)	P value*	P value†
Age (days)	127 ± 5	135 ± 4	148 ± 4	0.007	0.001
Tumor no. per mouse	58.9 ± 9.2	65.6 ± 6.5	42.1 ± 7.5	0.070	0.02
Tumor volume (mm^3) per mouse	177 ± 32	210 ± 23	95 ± 26	0.007	0.01
Tumor volume (mm^3) per tumor per mouse	8.8 ± 1.6	9.6 ± 1.2	3.1 ± 1.3	0.002	<0.0001

(DMEM) containing L-glutamine and supplemented with 10% FBS, 100 U/mL penicillin and 100 mg/mL streptomycin. When 80% confluent, cells were plated onto 24-well plates. Once 80% confluent again, the medium was replaced with fresh medium containing treatment compounds.

The amount of cell killing due to oxaliplatin (Sigma Chemical Company) was determined by analysing cells using 3-(4,5-dimethylthiazol-2-yl)-5(3-carboxymethoxphenyl)-2-(4-sulphophenyl)-2H-tetrazolium (Promega) and phenazine ethosulphate as an electron coupling reagent reduced by mitochondria to produce a chromophore with maximum absorption at 540 nm. HCT116 cells were cultured for 24 or 48 h in medium containing either oxaliplatin or oxaliplatin plus various concentrations of PBN. Treated cells were then washed twice with PBS and cell viability determined. Linearity with cell number was achieved at 25 min of incubation and therefore this time was used to estimate the proportion of live cells.

Statistics

Comparisons among treatment groups were made using ANOVA assuming unequal variances with $p < 0.05$ considered significant (JMP version 5.0.1, SAS, Cary, NC).

Results

Tumour enumeration

Three groups of $Apc^{Min/+}$ mice were treated with PBN, 4-OHPBN or sham and at necropsy a significant decrease in the total number of intestinal tumours, tumour volume per mouse and tumour volume per tumour per mouse was seen for the PBN group compared to the other groups (Table I). An increased weight gain was consistent with the lack of any sign of toxicity caused by administering either of the nitrones. Since anaemia from intestinal haemorrhage is the primary cause of death in this model, increased survival in the PBN group was likely due to lesser tumour burden. In contrast, no significant differences were found between the sham and 4-OH-PBN groups. This observation, *viz* that 4-OH-PBN was no different than sham, was unexpected and, compared to PBN, may have been due to the retrospective recognition that this compound had low solubility in water (see discussion).

When the average number of colon adenomas was analysed, no significant differences were found between shams and 4-OH-PBN-treated mice. Because we suspected that the 4-OHPBN-treated group had been under-treated and since the average number of colon adenomas in the $Apc^{Min/+}$ mice is typically less than five per mouse, we performed a post-hoc analysis that compared PBN-treated mice to combined data for sham- and 4-OHPBN-treated groups. Using these assumptions, PBN-treated mice showed a non-significant trend toward fewer average number of colon adenomas compared to controls (1.8 ± 0.3 vs 2.3 ± 0.2, $p > 0.05$), but tumour volumes (mm^3) were significantly decreased (17 ± 11 vs 55 ± 8, $p < 0.01$) as were adenoma volume (mm^3) per adenoma (26 ± 3.7 vs 6.9 ± 4.9, $p < 0.01$).

Percentage survival

PBN treatment was associated with significantly improved survival compared to the other groups. The percentage survival of mice in untreated, PBN-treated and 4-OH-PBN-treated mice are shown in Figure 1, which shows the PBN-treated animals with the best median survival of 152 days (all mice were sacrificed

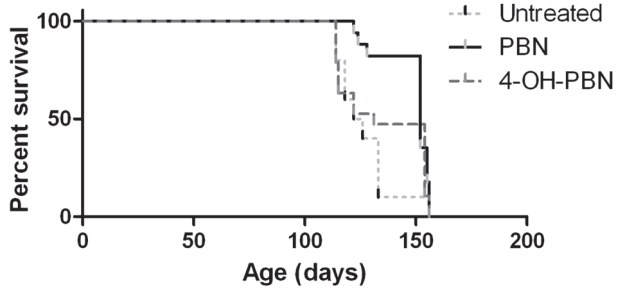

Figure 1. Calculation of percentage survival for non-treated, PBN-treated and 4-OH-PBN-treated mice over a period of 156 days of age when remaining mice were sacrificed. PBN-treated mice have increased percentage survival (n = 17; median survival 152 days with 35% surviving to 154 days) in comparison to non-treated mice (n = 10; median survival 124 days with 10% surviving to 154 days) and 4-OH-PBN-treated mice (n = 19; median survival 131 days with 11% surviving to 154 days).

at 156 days), with 35% of these mice still surviving at 154 days. Comparatively, the untreated mice with the worst survival had a median survival of 124 days, with only 10% surviving at 154 days; and the 4-OH-PBN-treated mice had a mean survival of 131 days, with 11% surviving at 154 days.

Morphological MRI assessment

To verify our ability to identify colon tumours by MRI, we tested a dual contrast method in several *Apc*$^{Min/+}$ mice using Ferumoxide instilled into the colon as a negative contrast agent and Gd-DTPA injected intravenously as a positive contrast agent. MRI scans showed that adenomas were readily detected in the wall of the colon (Figure 2). Next, a sub-set of sham and PBN- or 4-OHPBN-treated mice were followed longitudinally for 6–18 weeks of age for changes in colonic MRI signal intensity following Gd-DTPA administration. Analysis at 18 weeks was not feasible because too many sham- and 4-OHPBN-treated mice died between 16–18 weeks of age to permit valid comparisons. For other time points, the relative MRI signal intensities (referenced to back muscle) were measured for each colon image slice and all slices compiled to obtain a total colonic MRI signal intensity. Sham-treated mice showed a significant increase in MRI signal intensity over 7–16 weeks of age (Figure 3A, $p < 0.05$). In contrast, PBN treatment resulted in a significant decrease in MRI signal intensity (Figure 3B, $p < 0.05$). 4-OH-PBN treatment showed a non-significant decrease in MRI signal intensity ($p > 0.05$) and was not significantly different compared to shams ($p > 0.05$). Representative colon adenomas detected by contrast-enhanced MRI are illustrated in Figures 3D and E.

Finally, a second MRI analysis was performed on these same data using pixel values by an independent MRI group (Figure 4). Perfusion maps were used to depict Gd-DTPA uptake in colon adenomas with pixel values outlined for analysis (Figure 4D). The slopes across the three groups (untreated, PBN and 4-OH-PBN) were evaluated with respect to days of treatment. This produced an $F(2,123)$ of 6.44, which indicated significant differences between the regression coefficients ($p < 0.0055$). Consistent with prior findings, shams (untreated) showed a significant increase in MRI pixel values for colon adenomas over time (Figure 4A, $p < 0.05$). In contrast, nitrone-treated mice demonstrated decreased MRI pixel values over time, compared to shams, that were significant for both the PBN-treated group (Figure 4B, $p < 0.01$) and the 4-OH-PBN-treated

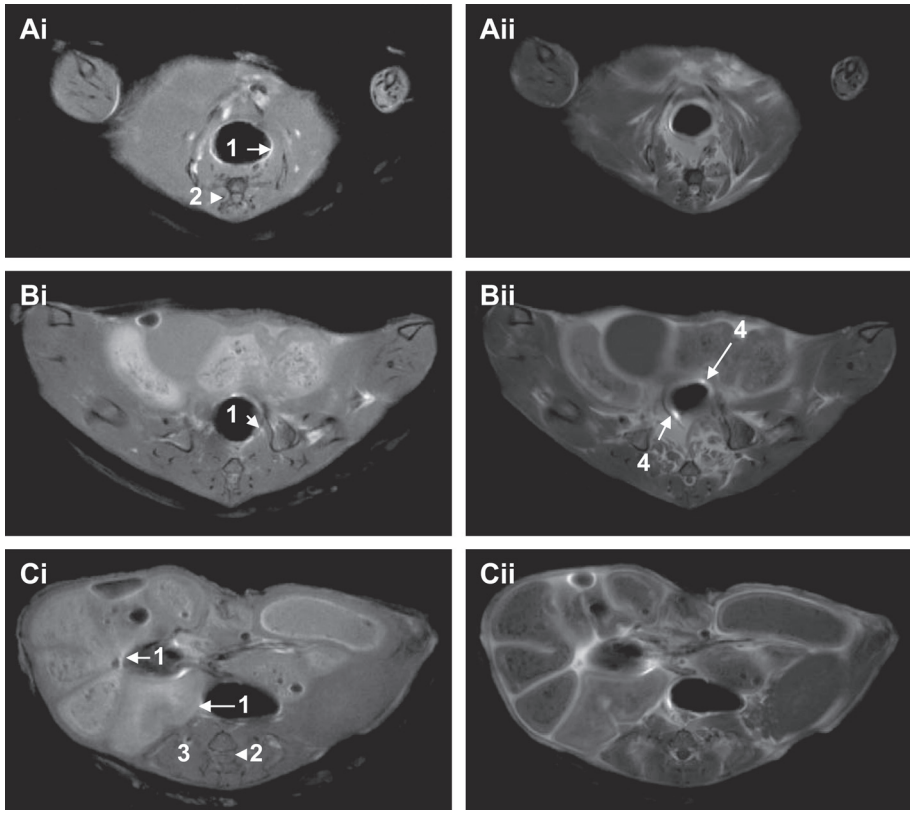

Figure 2. MRI of colon regions: (A) lower to mid-colon and (C) mid to upper colon of non-treated wild type mice in the supine position pre- (i) and post-contrast (ii) following administration of Ferumoxides by intra-colonic injection and intravenous Gd-DTPA via tail vein. Note that colon lumen (1) is better defined in contrast-enhanced images and that possible small adenomas are highlighted in Bii (4). Other anatomical features include the spinal cord and vertebrae (2), and back muscles (3). In the lower to mid-colon regions (A), peristalsis resulted in slight differences in co-registration of pre- and post-contrast images.

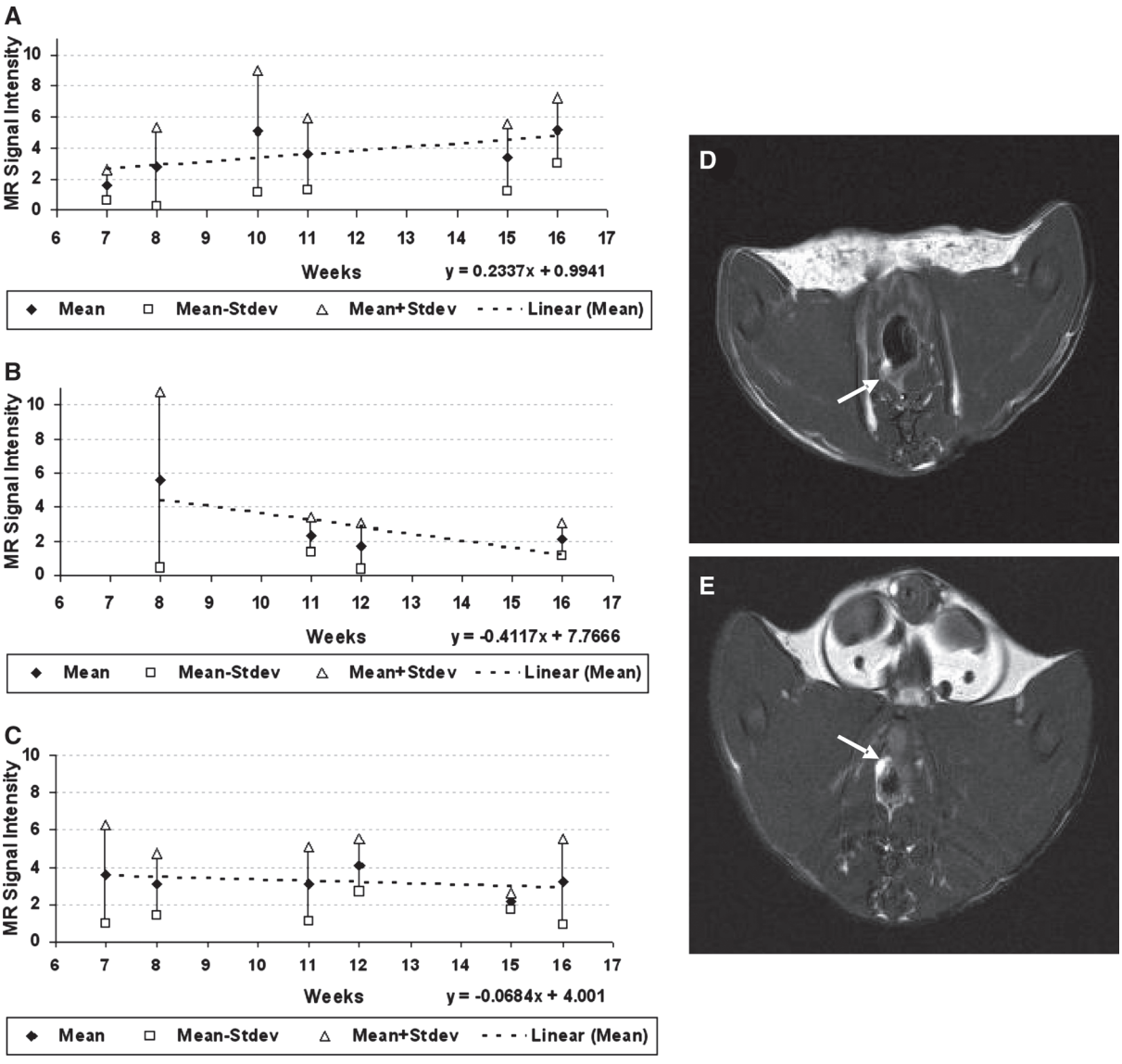

Figure 3. MRI signal intensity (A–C) from uptake of Gd-DTPA in colon adenomas in $Apc^{Min/+}$ mice that over 16 weeks were treated with (A) sham (n = 15), (B) PBN (n = 13) or (C) 4-OHPBN (n = 14). Note that PBN-treated mice show decreased MRI signal intensity compared to increased signals in sham-treated mice. MRI images (D and E) depict adenomas (arrow) that have taken up Gd-DTPA and have increased MRI signal intensities in a non-treated mouse. Linear slopes were calculated for each treatment group over 7–16 weeks of observation.

mice (Figure 4C, $p < 0.05$). Regarding 4-OH-PBN treatment, although the MR signal intensity analyses were not significantly different compared to shams (Figure 3C), a decreasing trend was apparent.

PBN effect on oxaliplatin killing of colon cancer cells

We next sought to determine the effect PBN on oxaliplatin-mediated killing of cancer cells. HCT116 colon cancer cells were treated with 10 μM oxaliplatin and after 2 days showed significant cell death (Table II). In contrast, PBN showed no significant effect on killing up to 1 mM. When PBN was combined with oxaliplatin, slight protection was noted against oxaliplatin toxicity at 2 mM PBN with a decrease relative to control from 29.3% to 24.7% at 2 mM. The effect of PBN on HCT116 cells at 2 mM was then tested across a range of oxaliplatin concentrations (0–20 μM). This concentration of PBN, in the absence of oxaliplatin, had no discernable toxic effects on HCT116 cells. When oxaliplatin was added to cells there was only slightly decreased susceptibility at the lower concentrations compared to oxaliplatin alone (Figure 5 Finally, we evaluated the effect of PBN on oxaliplatin-mediated apoptosis in HCT116 cells. HCT116 cells generated the active fragment of caspase 3 following treatment with oxaliplatin at 10 and 20 μM for 24 and 48 h (Figure 6). Addition of PBN at 2 mM slightly decreased the amount of active fragment caspase 3 for cells exposed to oxaliplatin at 24 h but showed no effect at 48 h.

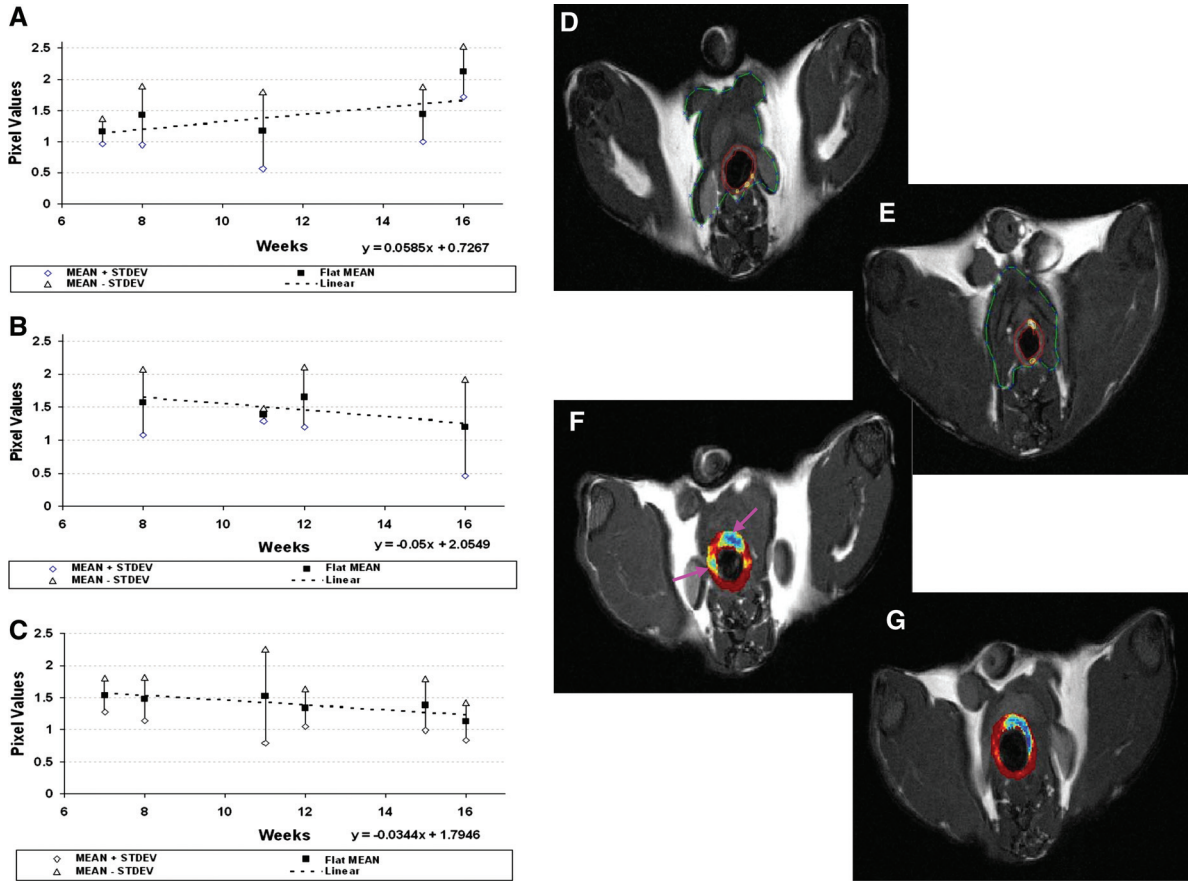

Figure 4. Calculation of MRI pixel values from perfusion maps obtained following Gd-DTPA uptake in (A) sham-treated, (B) PBN-treated and (C) 4-OH-PBN-treated mice from 7–16 weeks of age. (D) Perfusion map of Gd-DTPA uptake in adenomas (arrows). PBN- and 4-OH-PBN-treated mice show decreased pixel values in colon lumen compared to sham-treated mice.

Discussion

This study is the first to demonstrate the anti-cancer activity of orally administered PBN in the *Apc*$^{Min/+}$ model of intestinal neoplasia. The PBN-induced decrease in intestinal tumours (Table I) was confirmed by contrast-enhanced MRI studies of the colon (Figures 2 and 3). The MRI data also suggested that PBN maintained effectiveness throughout the treatment period, with a steady downward trend in colon tumour volume over 10 weeks of observation using this technique. In contrast, and as expected, sham-treated mice showed a gradual time-dependent increase in total colon MRI signal intensity (Figures 2B and 3B). These data indicate that PBN was able to diminish tumour volume in *Apc*$^{Min/+}$ mice over time—a therapeutic effect—and, by enumerating adenomas in both large and small intestines, also decrease the total number of adenomas—a preventive effect. The percentage survival data (Figure 1) supports the anti-cancer effect of PBN.

For 4-OH-PBN treatment, percentage survival data was not as strong as observed for PBN, but a slight increase in survivability was seen in comparison to shams. The discrepancies in these data (tumour enumeration, MRI evaluations and percentage survival) for 4-OH-PBN compared to shams was unexpected since 4-OH-PBN had been previously shown to have anti-cancer activity in the choline deficient model of liver cancer [4,6]. We should note, however, that in the liver cancer study 4-OH-PBN was administered as a dietary additive and not in drinking water as was done in this study. Because of differences in

Table 2. PBN effect on oxaliplatin (OXPN) killing of HCT-116 cells.

	Optical density of MTS reduction product		
PBN Added (mM)	Control no OXPN	Treated 10 μM OXPN	% Decrease relative to control
0	0.700 (±0.003)	0.495 (±0.006)	29.3
0.5	0.745 (±0.004)	0.498 (±0.023)	33.1
1.0	0.740 (±0.001)	0.536 (±0.002)	29.0
2.0	0.772 (±0.006)	0.581 (±0.014)	24.7

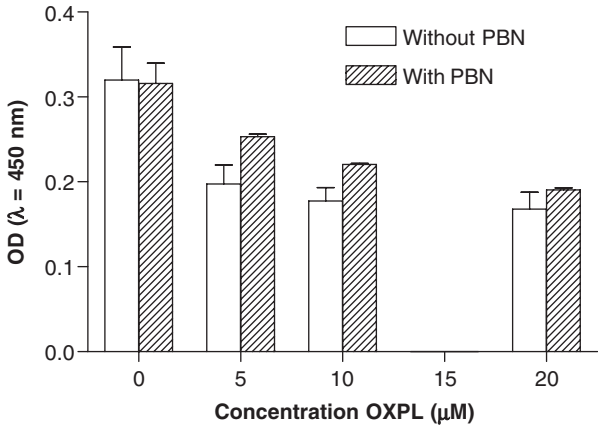

Figure 5. Killing of HCT116 cells at 48 h post-incubation by oxaliplatin in the presence of 2 mM PBN (shaded bars). Increased optical density is directly proportional to the number of live cells present.

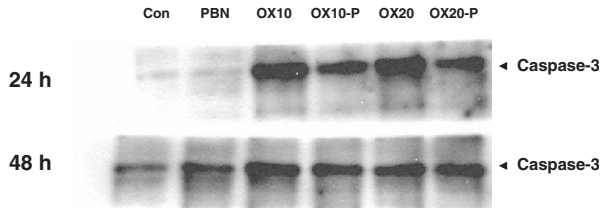

Figure 6. Western blotting of active fragment of caspase 3 in HCT116 cells treated with either 10 μM or 20 μM oxaliplatin or in the presence of 2 mM PBN (OX10-P; OX20-P).

route of administration and despite one authoritative publication indicating that 4-OH-PBN is more water-soluble than PBN [34], we retested the solubility of 4-OH-PBN and PBN to determine whether the route of administration might explain the discrepancy in 4-OH-PBN results. PBN proved to be readily soluble in drinking water to ~ 150 mM, a 35-fold higher concentration than needed to deliver 100 mg/kg-day as designed for this study. The maximum solubility of 4-OH-PBN, however, was only 500 μM, a concentration that provided only 13 mg/kg-day rather than 100 mg/kg-day as intended. The previously reported water solubility for 4-OH-PBN was based on data collected in an octanol/water partition experiment [34]. Under these conditions, large quantities of 4-OH-PBN were found in the aqueous phase, probably due to octanol-induced and micelle-enhanced solubility. In the present study, however, we only added a small amount of crystalline 4-OH-PBN to drinking water (37 mg per 100 mL) and failed to visually detect inadequate dissolution. This 10-fold smaller available dose of 4-OH-PBN likely explains the less than expected observations and the activity of this nitrone in *Apc*$^{Min/+}$ mice remains to be determined. Future studies using 4-OH-PBN may need to take into consideration alternative treatment preparations (e.g. different routes of administration).

After confirming the anti-cancer activity of PBN in the *Apc*$^{Min/+}$ model, we next wanted to determine whether PBN, as a representative nitrone, was compatible with at least one chemotherapeutic agent currently used in the treatment of CRC. We exposed a human CRC cell line with oxaliplatin and found that at a high concentration of PBN (2 mM) there was only a small suppressive effect on oxaliplatin killing. PBN also suppressed killing at lower oxaliplatin concentrations, although the overall effect was even smaller (Figure 5). To ascertain whether PBN altered apoptotic processes due to oxaliplatin killing, we measured the active fragment of caspase 3 at several oxaliplatin concentrations while PBN was fixed at 2 mM. The amount of caspase 3 active fragment at 24 and 48 h generally reflected the number of surviving cells as assessed by the MTS assay (data not shown). These data suggested that PBN had only a slight negative effect on oxaliplatin killing of cancer cells *in vitro* and this effect was enhanced at high PBN-to-oxaliplatin ratios. Perhaps at high concentration PBN decreases oxaliplatin uptake, although, by whatever mechanism, the effect appeared small when the ratio of PBN-to-oxaliplatin was 100:1 (2 mM PBN and 20 μM oxaliplatin). A concentration of 2 mM PBN is much higher than would be expected *in vivo* (~ 100 μM) and so little if any effect on oxaliplatin killing of cancer cells is anticipated *in vivo*, although this remains to be tested.

Three separate cancer models now show that PBN-related nitrones have broad anti-cancer activity. We initially discovered this property using a choline deficient model of liver cancer [3–6]. In those studies, PBN and 4-OHPBN demonstrated significant anti-cancer activity when administered in the diet. Similarly, PBN showed anti-cancer activity in the rat orthotopic (C6 cells) glioblastoma model [7]. These observations and the finding that PBN reduces tumour burden in the *Apc*$^{Min/+}$ model provide strong evidence for the potential of nitrones in cancer treatment and/or prevention.

The mechanistic basis for the anti-cancer activity of nitrones is unknown. Clearly PBN does not act as a classical cancer chemotherapeutic agent to directly kill cancer cells (Table II). One possible hypothesis involves the anti-inflammatory properties of these compounds [18]. Our group [35], along with Lala and Chakraborty [36] and Lirk et al. [37], reviewed the field and noted enhanced iNOS expression in many human tumours, including CRC, and for multiple experimental models of cancer including *Apc*$^{Min/+}$ mice [38]. Based on these findings and our own experimental observations [5,35,39], we speculate that PBN inhibits tumour growth by suppressing iNOS and NO [18]. Mechanisms by which NO might promote cancer are unclear, but the formation of S-nitrosylation adducts in key cysteines of essential proteins and enzymes is probably important [18]. For example, S-nitrosylation of caspases can inhibit apoptosis and prevent cancer cell death [40–42]. Data

from the choline deficient model of liver cancer supports such a mechanism. Our observations using this model show that PBN (1) decreased the size of pre-neoplastic liver lesions, (2) decreased iNOS and NO production in the liver and (3) enhanced apoptosis in pre-neoplastic 'islands', but not in cells of surrounding normal tissue [5]. These findings suggest that administering PBN decreases NO production and accelerates caspase-mediated apoptosis resulting in enhanced death of pre-neoplastic 'islands' [5].

Several animal models of intestinal neoplasia have demonstrated the importance of iNOS and NO in cancer development. In the azoxymethane-induced rat model, Rao et al. [30,43] showed that inhibition of iNOS slowed cancer development. Another approach using $Apc^{Min/+}$ mice produced similar supportive data [44]. In a study by Ahn and Ohshima [44], aminoguanidine, a specific iNOS inhibitor, administered in drinking water suppressed adenoma formation. These investigators also knocked out *Nos2*, the iNOS gene, and noted that $Apc^{Min/+}iNOS^{-/-}$ mice as well as $Apc^{Min/+}iNOS^{+/-}$ mice had significantly fewer adenomas than $Apc^{Min/+}iNOS^{+/+}$ mice. This observation clearly implicates iNOS and NO in the development of intestinal adenomas in this model.

Finally, COX-2, an inducible pro-inflammatory enzyme, is strongly associated with adenoma and CRC formation. Expression of COX-2 is also inhibited by PBN [45]. In previous work by our group, we showed that PBN suppressed COX-2 by inhibiting signal transduction [46]. In the choline deficient model of liver cancer, PBN also suppressed PGE_2, a downstream product of COX-2, but showed little effect on COX-2 mRNA or protein expression in the liver [5]. It should be noted that PBN levels in the liver are insufficient to alter the catalytic activity of COX-2. Recent studies indicate that NO from iNOS enhances COX-2 activity through S-nitrosylation of the protein [47]. Therefore, decreased COX-2 activity due to PBN could be, in part, the result of iNOS inhibition. We were unable to examine tumours from PBN-treated and control $Apc^{Min/+}$ mice for iNOS and COX-2 expression in this study, but this is an area for future investigation.

In summary, PBN, a prototypical nitrone, showed significant anti-cancer activity in the $Apc^{Min/+}$ model. Although 4-OH-PBN, a related nitrone, had less activity than PBN, this was likely related to the poor water-solubility of this compound and its efficacy remains to be established. These data indicate that nitrones are highly promising novel agents for the prevention and/or treatment of CRC.

Acknowledgements

Research was supported in part by Oklahoma Applied Research Support (OARS) grant AR052-041, NIH RO1CA82506, Oklahoma Center for the Advancement of Science & Technology (OCAST) fMRI.002, Department of Veterans Affairs Merit Review Program, and the Frances Duffy Endowment. Robert A. Floyd is Merrick Foundation Chair in Aging research. We thank Donna Howell for aid with graphics and document development.

Declaration of interest: The authors report no conflicts of interest. The authors alone are responsible for the content and writing of the paper.

References

[1] Horner MJ, Ries LAG, Krapcho M, Neyman N, Aminou R, Howlader N, Altedruse N, Feuer SF, Huang L, Mariotto A, Miller BA, Lewis DR, Eisner MP, Stinchomb DG, Edwards BK. SEER cancer statistics review. 1006. National Cancer Institute; 1975.

[2] Engstrom PF. Systemic therapy for advanced or metastatic colorectal cancer: National Comprehensive Cancer Network guidelines for combining anti-vascular endothelial growth factor and anti-epidermal growth factor receptor monoclonal antibodies with chemotherapy. Pharmacotherapy 2008;28: 18S–22S.

[3] Floyd RA, Kotake Y, Hensley K, Nakae D, Konishi Y. Reactive oxygen species in choline deficiency induced carcinogenesis and nitrone inhibition. Mol Cell Biochem 2002;234/235:195–203.

[4] Nakae D, Kishida H, Enami T, Konishi Y, Hensley KL, Floyd RA, Kotake Y. Effects of phenyl *N-tert*-butyl nitrone and its derivatives on the early phase of hepatocarcinogenesis in rats fed a choline-deficient, l-amino acid-defined diet. Cancer Sci 2003;94:26–31.

[5] Nakae D, Kotake Y, Kishida H, Hensley KL, Denda A, Kobayashi Y, Kitayama W, Tsujiuchi T, Sang H, Stewart CA, Tabatabaie T, Floyd RA, Konishi Y. Inhibition by phenyl *N-tert*-butyl nitrone on early phase carcinogenesis in the livers of rats fed a choline-deficient, L-amino acid-defined diet. Cancer Res 1998;58:4548–4551.

[6] Nakae D, Uematsu F, Kishida H, Kusuoka O, Katsuda S, Yoshida M, Takahashi M, Maekawa A, Denda A, KonishiY, Kotake Y, Floyd RA. Inhibition of the development of hepatocellular carcinomas by phenyl N-tert-butyl nitrone in rats fed with a choline-deficient, L-amino acid-defined diet. Cancer Lett 2004;206:1–13.

[7] Doblas S, Saunders D, Tesiram Y, Kshirsager P, Pye Q, Oblander J, Gordon B, Kosanke S, Floyd RA, Towner RA. Phenyl-tert-butyl-nitrone induces tumor regression and decreases angiogenesis in a C6 rat glioma model. Free Radic Biol Med 2007;44:63–72.

[8] Janzen EG. Spin trapping. Acc Chem Res 1971;4:31–40.

[9] Buettner GR. Spin trapping: ESR parameters of spin adducts. Free Radic Biol Med 1987;3:259–303.

[10] Janzen EG. A critical review of spin trapping in biological systems., In: unknown editor. Free radicals in biology. Academic Press, Inc.; 1980. p. 115–154.

[11] Mason RP, Chignell CF. Free radicals in pharmacology and toxicology—selected topics. Pharmacol Rev 1982;33: 189–211.

[12] Poyer JL, Floyd RA, McCay PB, Janzen EG, Davis ER. Spin trapping of the trichloromethyl radical produced during enzymic NADPH oxidation in the presence of carbon tetrachloride or carbon bromotrichloromethane. Biochim Biophys Acta 1978;539:402–409.

[13] Bolli R, McCay PB. Use of spin traps in intact animals undergoing myocardial ischemia/reperfusion: a new approach to

assessing the role of oxygen radicals in myocardial 'stunning'. Free Radic Biol Med 1990;9:3–6.
[14] Bolli R, Patel BS, Jeroudi MO, Lai EK, McCay PB. Demonstration of free radical generation on 'stunned' myocardium of intact dogs with the use of the spin trap a-phenyl N-tert-butyl nitrone. J Clin Invest 1988;82:476–485.
[15] Lai EK, Crossley C, Sridhar R, Misra HP, Janzen EG, McCay PB. *In vivo* spin trapping of free radicals generated in brain, spleen, and liver during gamma radiation of mice. Arch Biochem Biophys 1986;244:156–160.
[16] Mason RP. Assay of *in situ* radicals by electron spin resonance. Methods Enzymol 1983;105:416–421.
[17] Floyd RA. Protective action of nitrone-based free radical traps against oxidative damage to the central nervous system. Adv Pharmacol 1997;38:361–378.
[18] Floyd RA. Nitrones as therapeutics in age-related diseases. Aging Cell 2006;5:51–57.
[19] Maples KR, Green AR, Floyd RA. Nitrone-related therapeutics: potential of NXY-059 for the treatment of acute ischaemic stroke. CNS Drugs 2004;18:1071–1084.
[20] Floyd RA. Role of oxygen free radicals in carcinogenesis and brain ischemia. FASEB J 1990;4:2587–2597.
[21] Moser AR, Luongo C, Gould KA, McNeley MK, Shoemaker AR, Dove WF. ApcMin: a mouse model for intestinal and mammary tumorigenesis. Eur J Cancer 1995;31A:1061–1064.
[22] Aoki K, Taketo MM. Adenomatous polyposis coli (APC): a multi-functional tumor suppressor gene. J Cell Sci 2007;120: 3327–3335.
[23] Haigis KM, Hoff PD, White A, Shoemaker AR, Halberg RB, Dove WF. Tumor regionality in the mouse intestine reflects the mechanism of loss of Apc function. Proc Natl Acad Sci USA 2004;101:9769–9773.
[24] Levy DB, Smith KJ, Beazer-Barclay Y, Hamilton SR, Vogelstein B, Kinzler KW. Inactivation of both APC alleles in human and mouse tumors. Cancer Res 1994;54:5953–5958.
[25] Moser AR, Dove WF, Roth KA, Gordon JI. The Min (multiple intestinal neoplasia) mutation: its effect on gut epithelial cell differentiation and interaction with a modifier system. J Cell Biol 1992;116:1517–1526.
[26] Shoemaker AR, Moser AR, Dove WF. N-ethyl-N-nitrosourea treatment of multiple intestinal neoplasia (Min) mice: age-related effects on the formation of intestinal adenomas, cystic crypts, and epidermoid cysts. Cancer Res 1995;55:4479–4485.
[27] Oshima M, Oshima H, Kitagawa K, Kobayashi M, Itakura C, Taketo M. Loss of Apc heterozygosity and abnormal tissue building in nascent intestinal polyps in mice carrying a truncated Apc gene. Proc Natl Acad Sci USA 1995;92:4482–4486.
[28] Jacoby RF, Marshall DJ, Newton MA, Novakovic K, Tutsch K, Cole CE, Lubet RA, Kelloff GJ, Verma A, Moser AR, Dove WF. Chemoprevention of spontaneous intestinal adenomas in the Apc Min mouse model by the nonsteroidal anti-inflammatory drug piroxicam. Cancer Res 1996;56:710–714.
[29] Jacoby RF, Seibert K, Cole CE, Kelloff G, Lubet RA. The cyclooxygenase-2 inhibitor celecoxib is a potent preventive and therapeutic agent in the min mouse model of adenomatous polyposis. Cancer Res 2000;60:5040–5044.
[30] Rao CV, Cooma I, Rodriguez JG, Simi B, El Bayoumy K, Reddy BS. Chemoprevention of familial adenomatous polyposis development in the APC(min) mouse model by 1,4-phenylene bis(methylene)selenocyanate. Carcinogenesis 2000;21: 617–621.

This paper was first published online on Early Online on 19 October 2009

[31] Towner RA, Foley LM, Painter DM. Hepatocarcinogenesis tumor grading correlated with *in vivo* image-guided ^{1}H-NMR spectroscopy in rat model. Toxicol Appl Pharmacol 2005; 207:237–244.
[32] Towner RA, Hashimoto H, Summers PM. Non-invasive *in vivo* magnetic resonance imaging assessment of acute aflatoxin B1 hepatotoxicity in rats. Biochim Biophys Acta 2000;1475:314–320.
[33] Huie R, Cherry WR. Facile one-step synthesis of phenyl-tert-butylnitrone (PBN) and its derivatives. J Org Chem 1985;50:1531–1532.
[34] Janzen EG, West MS, Kotake Y, DuBose CM. Biological spin trapping methodology. III. octanol-water partition coefficients of spin-trapping compounds. J Biochem Biophys Methods 1996;32:183–190.
[35] Floyd RA, Kotake Y, Towner RA, Guo W-X, Nakae D, Konishi Y. Nitric oxide and cancer development. J Toxicol Pathol 2007;20:77–92.
[36] Lala PK, Chakraborty C. Role of nitric oxide in carcinogenesis and tumour progression. Lancet Oncol 2001;2:149–156.
[37] Lirk P, Hoffmann G, Rieder J. Inducible nitric oxide synthase—time for reappraisal. Curr Drug Targets Inflamm Allergy 2002;1:89–108.
[38] Yagihashi N, Kasajima H, Sugai S, Matsumoto K, Ebina Y, Morita T, Murakami T, Yagihashi S. Increased in situ expression of nitric oxide synthase in human colorectal cancer. Virchows Arch 2000;436:109–114.
[39] Kotake Y, Kishida H, Nakae D, Floyd RA. Nitric oxide production by primary liver cells isolated from amino acid diet fed rats. Methods Enzymol 2005;396:535–541.
[40] Radisavljevic Z. Nitric oxide suppression triggers apoptosis through the FKHRL1 (FOXO3A)/ROCK kinase pathway in human breast carcinoma cells. Cancer 2003;97: 1358–1363.
[41] Salvucci O, Carsana M, Bersani I, Tragni G, Anichini A. Antiapoptotic role of endogenous nitric oxide in human melanoma cells. Cancer Res 2001;61:318–326.
[42] Torok NJ, Higuchi H, Bronk S, Gores GJ. Nitric oxide inhibits apoptosis downstream of cytochrome *c* release by nitrosylating caspase 9. Cancer Res 2002;62:1648–1653.
[43] Rao CV, Indranie C, Simi B, Manning PT, Connor JR, Reddy BS. Chemopreventive properties of a selective inducible nitric oxide synthase inhibitor in colon carcinogenesis, administered alone or in combination with celecoxib, a selective cyclooxygenase-2 inhibitor. Cancer Res 2002;62: 165–170.
[44] Ahn B, Ohshima H. Suppression of intestinal polyposis in $Apc^{Min/+}$ mice by inhibiting nitric oxide production. Cancer Res 2001;61:8357–8360.
[45] Kotake Y, Sang H, Miyajima T, Wallis GL. Inhibition of NF-kB, iNOS mRNA, COX2 mRNA, and COX catalytic activity by phenyl-*N*-*tert*-butylnitrone (PBN). Biochim Biophys Acta 1998;1448:77–84.
[46] Tabatabaie T, Vasquez AM, Moore DR, Floyd RA, Kotake Y. Direct administration of interleukin-1 and interferon-g to rat pancreas leads to the *in vivo* production of nitric oxide and expression of inducible nitric oxide synthase and inducible cyclooxygenase. Pancreas 2001;23:316–322.
[47] Kim SF, Huri DA, Snyder SH. Inducible nitric oxide synthase binds, S-nitrosylates, and activates cyclooxygenase-2. Science 2005;310:1966–1970.